Optimum Optical and Electrical Filter Characteristics in Optically Preamplified Direct Detection (N)RZ Receivers

Martin Pfennigbauer, Peter J. Winzer, Martin M. Strasser, and Walter R. Leeb

Institut für Nachrichtentechnik und Hochfrequenztechnik, Technische Universität Wien, Gusshausstraße 25/389, A-1040 Wien, Austria

ABSTRACT

We give optimum values for the bandwidths of realistic optical and electrical filters (optical Fabry-Pérot filters and fiber Bragg gratings, electrical Bessel filters and first order RC low pass filters), as well as for realistic NRZ and (33% duty cycle) RZ input pulses for a free space laser communication system employing an optical booster and a direct detection receiver with optical preamplification. Different extinction ratios, the presence of background radiation, and the influence of the booster amplifier's amplified spontaneous emission (ASE) are emphasized. Our results show that the optimum optical filter bandwidth (both for NRZ and RZ) has to be sought in the range of 1.5 to 3 times the data rate. Using the optimum filter bandwidths, RZ coding yields a sensitivity improvement of up to $1.5dB$ compared to NRZ transmission. For typical system parameters and link distances higher than several thousand kilometers the booster ASE becomes less important than strong background radiation, while it causes severe sensitivity degradations for shorter distances.

Keywords: free space laser communications, optical intersatellite links, direct detection, optically preamplified receivers, NRZ, RZ, optical/electrical filtering, inter symbol interference.

1. INTRODUCTION

Recent developments towards space borne laser communication systems have pointed out that direct detection receivers combined with optical preamplification are a good choice for high data rate intersatellite links: The sensitivity of such direct detection receivers (i.e. the required number of photons per bit for a specified bit error probability) can be the *same* as that of coherent receivers employing heterodyne reception.[1] Concerning design effort, robustness, and availability of system components, direct detection receivers can also compete with coherent receivers.

In the past, the optical bandpass filter following the optical amplifier in optically preamplified direct detection receivers was chosen as narrow as possible to reduce the amplified spontaneous emission power at the detector. Owing to technological constraints, this was still much broader than the bandwidth of the data signal. However, (i) the increase of data rates into the $10-40Gbit/s$ range, (ii) the growing availability of optical filters with bandwidths down to about $10GHz$, and (iii) the employment of return-to-zero (RZ) coding have led to technically realizable situations in which too narrow optical filter bandwidths start to deteriorate receiver performance.

In this paper we present simulation results of investigations on free space intersatellite communication systems with fiber boosted transmitters and fiber preamplified direct detection receivers. The aim of the work is to assess the influence of filter characteristics (transfer function and bandwidth) for the receiver part of the system. For the bandwidth of the optical filter, a tradeoff is to be made between allowing incoherent light (background radiation plus amplified spontaneous emission (ASE) from booster and optical preamplifier) to reach the detector on one hand and degrading the signal on the other. For the bandwidth of the electrical low pass filter following the detector, the tradeoff is between spoiling the signal by letting too much noise pass a filter with a too high cut-off frequency and, too, signal degradation. Thus the optical and electrical filters have to be optimized together.

We include the influence of the booster amplifier's ASE and the background radiation of celestial bodies on the system performance. This leads to a distance-dependent effective receiver noise figure.

For further author information:
Tel.: +43-1-58801-38901
Fax: +43-1-58801-38999
e-mail: martin.pfennigbauer@ieee.org

In Section 2 we discuss the modeled system, which takes into account the signal pulse shape and filter transfer functions. Section 3 describes the simulation method. The simulation results are presented in Section 4. Section 5 summarizes our work.

2. SYSTEM MODEL

The system under consideration is depicted in Figure 1. It consists of an optical data source, a booster amplifier to amplify the transmit signal, a free space transmission section, and an optically preamplified direct detection receiver. It is the properties of the latter, on which this paper is focussed. The transmitter is characterized by its transmit field $e_t(t)$, assumed to be chirp-free, and the booster amplifier's gain G_b and noise figure F_b. The optical transmit field $e_t(t)$ is given by a sequence of $\cos^2(t)$-shaped pulses at a data rate R. The optical power $p_t(t)$ is normalized such that $p_t(t) = |e_t(t)|^2$. The optical power waveform representing a single '1'-bit $p_1(t)$ is specified within the interval $[0, (1+\eta)T_p]$ as

$$p_1(t) = \begin{cases} \frac{E_1}{2T_p}\left[1 - \sin\left(\frac{\pi}{\eta T_p}\left(\left|t - (1+\eta)\frac{T_p}{2}\right| - \frac{T_p}{2}\right)\right)\right], & t \,\epsilon\, \{[0, \eta T_p] \vee [T_p\,, (1+\eta)T_p)]\} \\ \frac{E_1}{T_p}, & t \,\epsilon\, [\eta T_p\,, T_p]\,, \end{cases} \tag{1}$$

where E_1 denotes the optical energy for a '1'-bit, T_p is the effective pulse duration,

$$T_p = \frac{\int_{-\infty}^{\infty} p_1(t)\mathrm{d}t}{\max\limits_t\{p_1(t)\}} = \frac{E_1}{\max\limits_t\{p_1(t)\}}\,, \tag{2}$$

and the parameter η specifies the pulse shape: Varying η from 1 to 0, the pulse changes from $\cos^2(t)$-like to rectangular. Setting T_p equal to the bit duration T leads to NRZ signals. By reducing the pulse duration to a fraction of the bit duration $T_p = d{\cdot}T$ with $d \leq 1$ being the duty cycle, RZ coding is covered. In this work we chose the realistic values of $\eta = 0.4$ for NRZ-pulses and $\eta = 1$ for 33% duty cycle RZ coding. The respective eye diagrams at the transmitter are shown in Fig. 1. Imperfect modulation results in a finite extinction ratio, ζ, which is, for the NRZ-case, defined as the ratio of the maximum optical power for a '1'-bit to the minimum optical power for a '0'-bit. For the RZ signal, ζ is defined as the ratio of the peak power for a one bit to the peak power of the not completely suppressed pulse for a '0'-bit, which is appropriate for pulse-train modulated RZ-signals.[2]

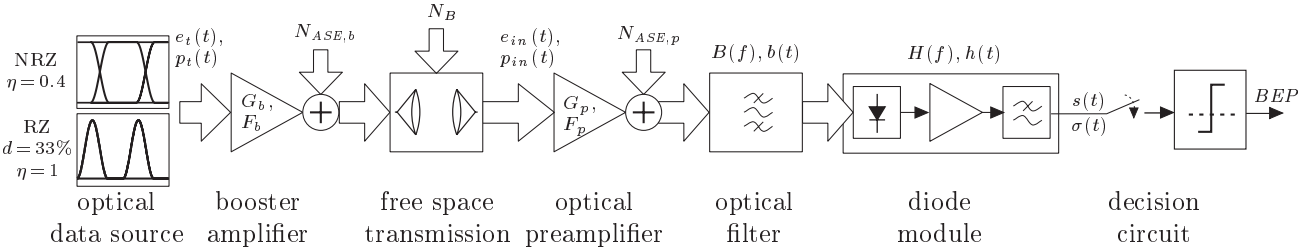

Figure 1. System model

The transmit booster and the optical preamplifier introduce a Gaussian noise process called amplified spontaneous emission (ASE), with power spectral density[3]

$$N_{ASE,b,p} = \frac{hc}{2\lambda} G_{b,p} F_{b,p} \tag{3}$$

per spatial (and polarization) mode, where hc/λ represents the photon energy (h being Planck's constant), λ denotes the laser wavelength, and $G_{b,p}$ and $F_{b,p} \geq 2$ are the optical amplifiers' gain and noise figure, respectively. The value of (3) doubles if two polarization modes have to be considered. For the calculations leading to the results presented here, it is assumed that no polarization filter is employed. (Since a well-designed receiver will be typically limited by the beat noise between signal and independent background radiation, a polarization filter would not make much difference in practice.)

Apart from booster and preamplifier ASE, there will also be noise at the receiver input caused by celestial bodies which are in the receive-telescope's field of view.[4] This background noise is represented by its power spectral density per (polarization) mode, N_B. The ASE of the booster amplifier and the background radiation are amplified by the preamplifier's gain. Both the transmitted signal and the booster ASE are attenuated by free space transmission. The signal power and the booster ASE density arriving at the receiver are given, as an approximation for the antennas operating in their mutual far fields, by[5,6]

$$p_{in} \approx \frac{0.41 p_t D_{TX}^2 D_{RX}^2}{r^2 \lambda^2} \tag{4}$$

and

$$N_{ASE,b,received} \approx \frac{0.2 hc G_b F_b D_{TX}^2 D_{RX}^2}{r^2 \lambda^3}, \tag{5}$$

where D_{TX} and D_{RX} are the transmit and receive telescope diameters and r is the link distance. Introducing a free space attenuation

$$L(r) \approx \frac{r^2 \lambda^2}{0.41 D_{TX}^2 D_{RX}^2} \tag{6}$$

leads to

$$N(r) = G_p \left[\frac{N_{ASE,b}}{L(r)} + N_B \right] + N_{ASE,p} = \frac{hc}{2\lambda} G_p F_{equiv}(r), \tag{7}$$

for the background power spectral density coupled to the receiver. This equation defines the (link distance dependent) *equivalent receiver noise figure*,

$$F_{equiv}(r) = \frac{G_b}{L(r)} F_b + N_B \frac{2\lambda}{hc} + F_p; \tag{8}$$

it represents all background noise terms (total incoherent light), i.e. booster ASE, background radiation and optical preamplifier ASE at the output of the receiver preamplifier.

After preamplification, the received signal is optically bandpass filtered to spectrally truncate the optical noise. The bandpass filter is assumed to be either a Fabry-Pérot filter (FPF) or a fiber Bragg grating (FBG) (in combination with a circulator to convert its bandstop characteristic into a bandpass characteristic) and is represented by its complex baseband field transfer function $B(f)$ and its complex baseband impulse response $b(t)$. We used the transfer functions

$$B_{FPF}(f) = \frac{1}{1 + j2f/FWHH} \tag{9}$$

for the Fabry-Pérot filter with $FWHH$ (full width half height), the $3dB$-bandwidth of the filter, and

$$B_{FBG}(f) = \frac{1}{\tan[\kappa l]} \cdot \frac{-j\kappa \sin[\beta(f) l]}{j\beta(f) \cos[\beta(f) l] - (2\pi f / v_g) \sin[\beta(f) l]}, \tag{10}$$

for the fiber Bragg grating,[7,8] where $\beta(f)$ stands short for

$$\beta(f) = \sqrt{(2\pi f / v_g)^2 - \kappa^2}\,, \tag{11}$$

and κ is the grating's coupling coefficient. In our simulations, κ was kept constant at a typical value[7] of $6cm^{-1}$, while the length of the grating, l, and the group velocity, v_g, were appropriately set to achieve the desired $FWHH$ at a constant sidelobe suppression ratio of $7dB$. Figure 2 shows magnitude and phase of the filter transfer functions.

For a qualitative assessment of the effect of the optical bandpass on the ASE, the *power equivalent width*

$$B_n = \int_{-\infty}^{+\infty} |B(f)|^2 df \tag{12}$$

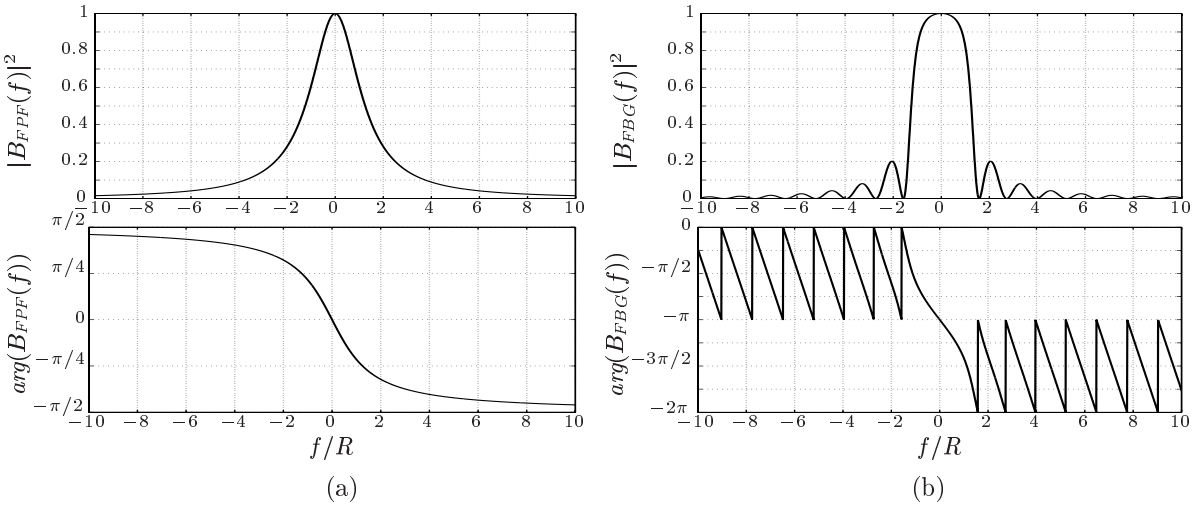

Figure 2. Squared magnitude and phase of the baseband field transfer function of a Fabry-Pérot filter (a) and of a fiber Bragg filter (b).

can be defined. Assuming the usable (data-) bandwidth to be equal to the filters' $FWHH$, the ratio $FWHH/B_n$ is a measure for the effectiveness of the filters' noise suppression. For the FPF the ratio of signal width to power equivalent width is 63.7% while it is 85.7% for a FBG. This explains why Bragg gratings can lead to higher receiver sensitivities than Fabry-Pérot filters (see Sect. 4.1).

The filtered optical signal is then converted into an electrical signal by the diode module consisting of a pin-diode, an amplifier and an electrical low-pass filter. For the overall transfer characteristics of the receive electronics $H(f)$, two cases were considered: a 5^{th} order Bessel or a 1^{st} order RC low pass characteristics. Bessel filters are often used because of their advantageous properties concerning low overshoot and the widely linear group velocity (and therefore low pulse broadening). The transfer functions of the filters are given by[9] (see Fig. 3)

$$H_{Bessel}(f) = \frac{945}{jf^5 + 15f^4 - 105jf^3 - 420f^2 + 945jf + 945} \tag{13}$$

and

$$H_{low\ pass}(f) = \frac{1}{1 + jf/B_{3dB}}. \tag{14}$$

As in the case of the optical filter, a power equivalent width can be defined. If $h(t)$ is normalized to unit area, $\int_{-\infty}^{\infty} h(t)dt = H(0) = 1$, it is written as

$$B_h = \int_0^{\infty} |H(f)|^2 df. \tag{15}$$

For the RC low pass the $3dB$ bandwidth B_{3dB} is related to B_h by $B_{3dB} = 2B_h/\pi$ while for the Bessel filter the 3dB bandwidth follows $B_{3dB} = 0.96B_h$.

Other parameters of the receiver electronics affecting system performance are the photo diode conversion gain S $[A/W]$ and the diode module's noise current density N_e $[A^2/Hz]$. The detected electrical signal is finally sampled, and a decision circuit produces a bit sequence to which a bit error probability (BEP) is assigned.

3. SIMULATION METHOD

The results presented here were obtained by means of a quasi-analytical approach: A pseudo random bit sequence (PRBS) with length $N = 2^7 - 1$ with "1"-bit pulses with power envelope defined by (1) was generated. The PRBS

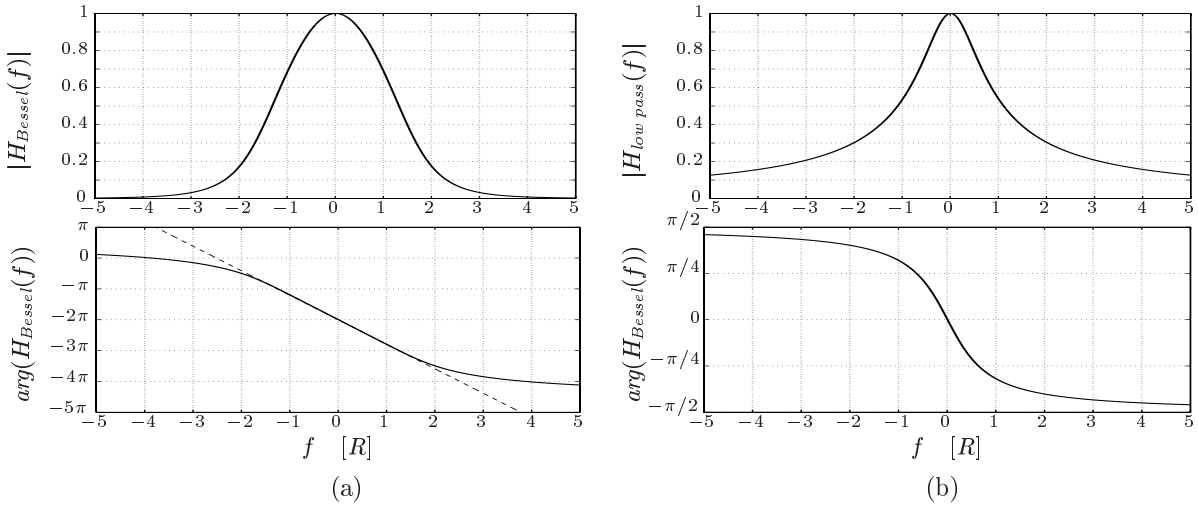

Figure 3. Magnitude and phase of Bessel 5^{th} order (a) and low pass filter 1^{st} order (b) transfer function. Note the widely linear phase of the Bessel filter.

length was chosen as a compromise between including all possible intersymbol interference (ISI) combinations and avoiding excessive simulation time. The electrical signal's mean at the decision gate, $s(t)$, follows from

$$s(t) = \frac{G_b}{L(r)} G_p S |(e_t * b)(t)|^2 * h(t), \tag{16}$$

with the impulse response of the optical and electrical filter $b(t)$ and $h(t)$ and $*$ denoting a convolution.

Concerning the noise terms, the beat terms of signal and incoherent light, $\sigma^2_{s-\mathrm{incoh}}$, and incoherent light with itself, $\sigma^2_{\text{incoh-incoh}}$, as well as the noise of the diode module's electronics were considered. For the calculation of the variances, the exact semi-classical noise terms[10] were implemented. The variance of the electronics' noise reads

$$\sigma^2_{elec} = N_e B_h. \tag{17}$$

The bit error probability was calculated by averaging the error probability of each single bit over the PRBS, i.e.

$$BEP = \frac{1}{N} \sum_{k=1}^{N} BEP_k, \tag{18}$$

with BEP_k being the error probability of one single bit

$$BEP_k = \mathcal{Q}\left(\frac{\pm(s(k/R + t_s) - s_{th})}{\sqrt{\sigma^2_{s-incoh}(k/R + t_s) + \sigma^2_{incoh-incoh} + \sigma^2_{elec}}} \right). \tag{19}$$

Here, $\mathcal{Q}$ is the complementary probability density function for Gaussian processes

$$\mathcal{Q}(x) = \frac{1}{2\pi} \int_x^\infty e^{-\alpha^2/2} d\alpha, \tag{20}$$

The sign "+" has to be used when detecting a '1', "−" when the bit under consideration is a '0'. Decision threshold s_{th} and sampling instant t_s are optimized with respect to *BEP*.

The quantity of ultimate interest is the receiver's sensitivity. Here, the sensitivity n_s is defined as the average number of photons per bit necessary at the input of the optical preamplifier to achieve $BEP = 10^{-9}$. Most of the results in this paper are given in terms of a sensitivity penalty γ_q relative to the quantum limit n_q, which is 41.0 photons per bit for optically preamplified direct detection receivers employing the Gaussian approximation,[11,12]

$$\gamma_q = 10 \log(n_s / n_q) \quad [dB]. \tag{21}$$

4. SIMULATION RESULTS AND DISCUSSION

4.1. Influence of filter characteristics on receiver sensitivity

We calculated the receiver sensitivity penalty γ_q for four combinations of optical and electrical filter characteristics (FPF–Bessel, FPF–RC low pass, FBG–Bessel and FBG–RC low pass). The optical bandwidth $FWHH$ and the electrical bandwidth B_h are independent variables. A link distance of $r = 5\,000km$ was assumed. This is a typical value for low earth orbit (LEO) multi-satellite systems. For the background radiation we chose $N_B = 10^{-20}W/Hz$, which is the case when the receive telescope looks directly into the sun.[4] The diameters of the telescopes were set to $D_{TX} = D_{RX} = 10cm$. Gain and noise figure of the booster and preamplifier were set to $G_b = 33dB$, $F_b = 5dB$, $G_p = 28dB$ and $F_p = 3dB$, which leads to an equivalent noise figure of $F_{equiv} = 3.3dB$. Figure 4 shows the sensitivity penalty γ_q vs. filter bandwidths for the four filter combinations for NRZ signals with a shape factor $\eta = 0.4$. For the time being, we neglect the electronics' noise (but see end of this subsection) and assume infinite extinction ratio ($N_e = 0$, $\zeta = \infty$). The contour lines are separated by $0.25dB$. The absolute minimum is marked by a cross. The resolution of the diagrams is $0.5R$ for the optical $FWHH$ and $0.1R$ for the electrical B_h.

One interesting effect common to all filter setups is that for too large bandwidths (optical as well as electrical), the penalty increases only moderately, whereas the sensitivity decreases dramatically for too narrow filters. The reason for the latter is – for NRZ – mainly intersymbol interference and subsequent eye closure, as well as increased '0'-bit signal dependent noise. For RZ, the reason has to be sought in signal energy rejection by the optical filter.[12]

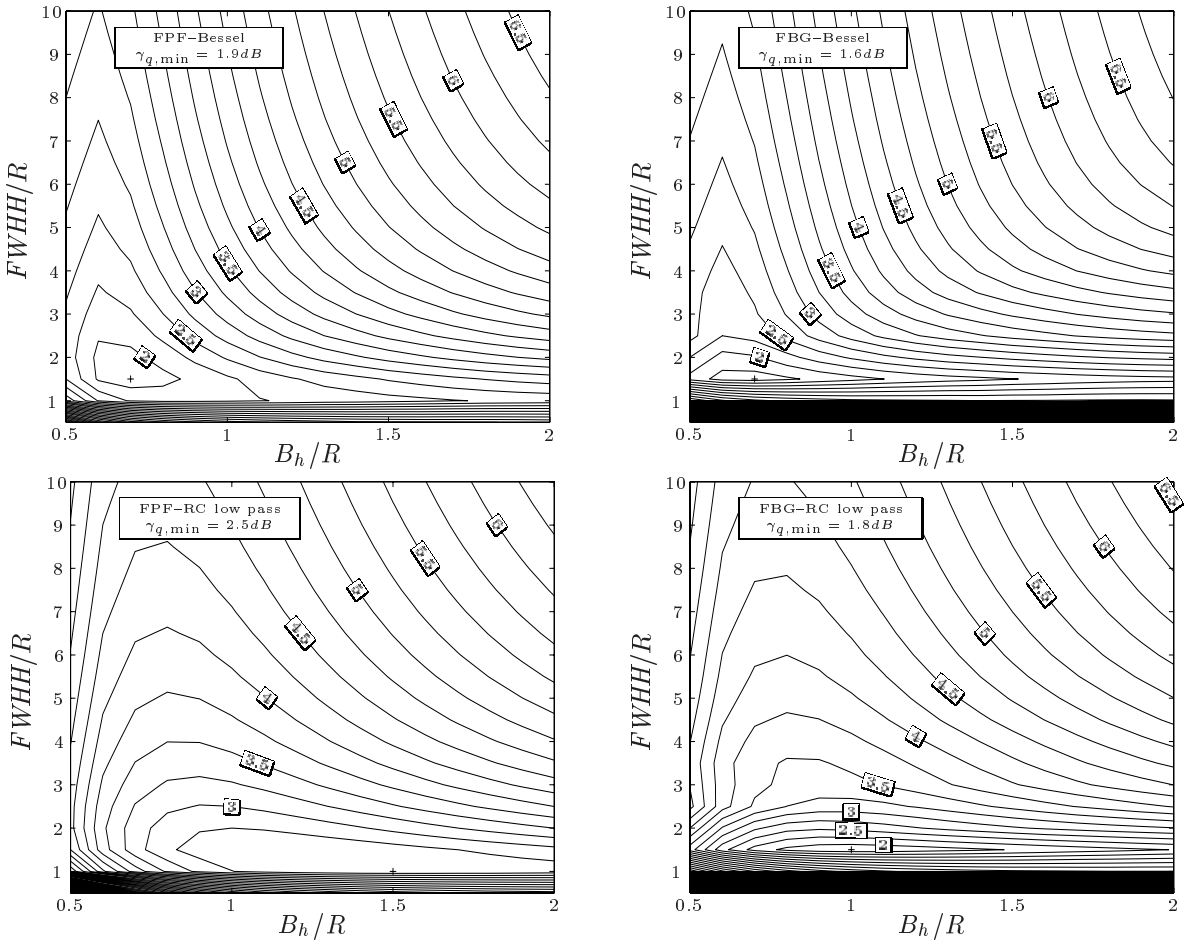

Figure 4. NRZ coding. Contour lines of the receiver sensitivity relative to the quantum limit as a function of optical $3dB$ bandwidth $FWHH$ and electrical power equivalent width B_h, both normalized to the data rate R. The four subplots represent different receiver setups as indicated by the insets. In all diagrams the contour lines are separated by $0.25dB$.

If the filter bandwidths are increased beyond the optimum, too much noise passes the filters, thus degrading the bit error probability. Comparison of the four subplots shows that with the combination of a fiber Bragg grating and a Bessel filter the best performance can be accomplished. This reflects the qualitative findings of Sect. 2. Concerning performance degradation due to off-optimum bandwidths, however, using a fiber Bragg grating is more critical. This can easily be understood considering the steep edges of the fiber Bragg grating compared those of the Fabry-Pérot filter (see Fig. 2).

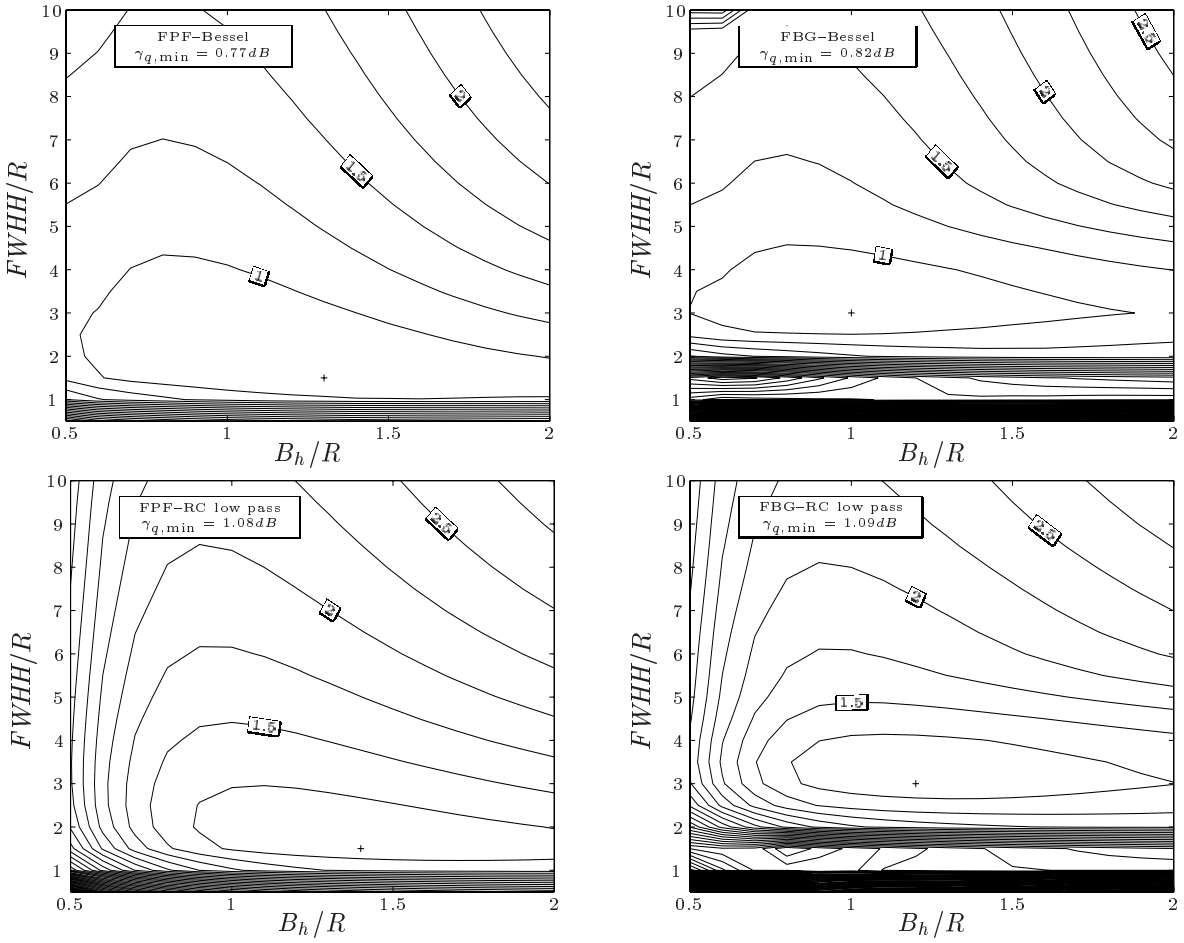

Figure 5. As Fig. 4, but for RZ coding with a duty cycle of $d = 0.33$ and a shape factor $\eta = 1$.

Figure 5 shows the sensitivity penalty for RZ signals with a duty cycle of $d = 33\%$ and a shape factor of $\eta = 1$. There are two significant differences to the results for NRZ: First, the achievable sensitivity is better for RZ signals than for NRZ signals. Second, the contour lines (again separated by $0.25dB$) are farther apart. Hence, RZ is less critical concerning optimum filter bandwidths. The achievable sensitivity improvement due to RZ coding, also called *RZ gain*, is in the range of $0.8dB$ to $1.4dB$, depending on the filter setup. (Higher values of up to $3.5dB$ for the RZ gain are obtained when not so steep NRZ pulses (e.g. $\eta = 1$) are taken as a baseline.) Even for filter bandwidths optimized for NRZ there is an RZ gain of about $0.5dB$, although the shorter RZ pulses are remarkably broader in the frequency domain. The reason is that RZ coded signals spectrally better exploit the electrical filter's transfer function than NRZ pulses. Another interesting aspect is that for the spectrally much broader RZ pulses, the optimum optical filter bandwidths are about the same; there are cases when RZ even asks for *smaller* bandwidths then NRZ. The reason is that RZ pulses (in contrast to NRZ) are not effected by ISI but rather by signal energy rejection by too narrow optical bandwidths, setting in when the optical filter bandwidth approaches the data rate.[12] One consequence of the higher spectral width of RZ pulses is that a Fabry-Pérot filter – with the less steep transfer function – yields slightly better performance than a fiber Bragg filter, in contrast to the NRZ case.

Taking into account electronic noise leads to some performance degradation and to a tendency towards somewhat higher optical and lower electrical optimum bandwidths.[12] The realistic value of $\sqrt{N_e} = 25pA/\sqrt{Hz}$ for the equivalent noise current density leads to an additional sensitivity penalty of about $0.7dB$, independent of signal and filter characteristics.

4.2. Influence of communication distance

Figure 6 shows the receiver sensitivity penalty γ_q vs. the communication distance r. The eight curves represent the possible filter combinations for both NRZ and RZ coding. Electronics noise is neglected and infinite extinction ratio is assumed. The background radiation is, again, assumed to be $N_B = 10^{-20}W/Hz$. The filter bandwidths were chosen optimum for each filter setup at the values determined in Sect. 4.1. The increase in penalty for small link distances is due to the booster amplifier's ASE. For the parameters used here, it can be neglected for distances greater than $5\,000km$. For typical intersatellite link setups (low earth orbit, LEO: $5\,000km$ and geostationary earth orbit, GEO: $80\,000km$) only background radiation and noise generated in the receiver have significant influence on the sensitivity. Zero background radiation would lower the presented curves by $0.4dB$. The different filter combinations yield the same behavior when r is varied. Simulations have shown that the optimum bandwidths are insensitive to link distance.

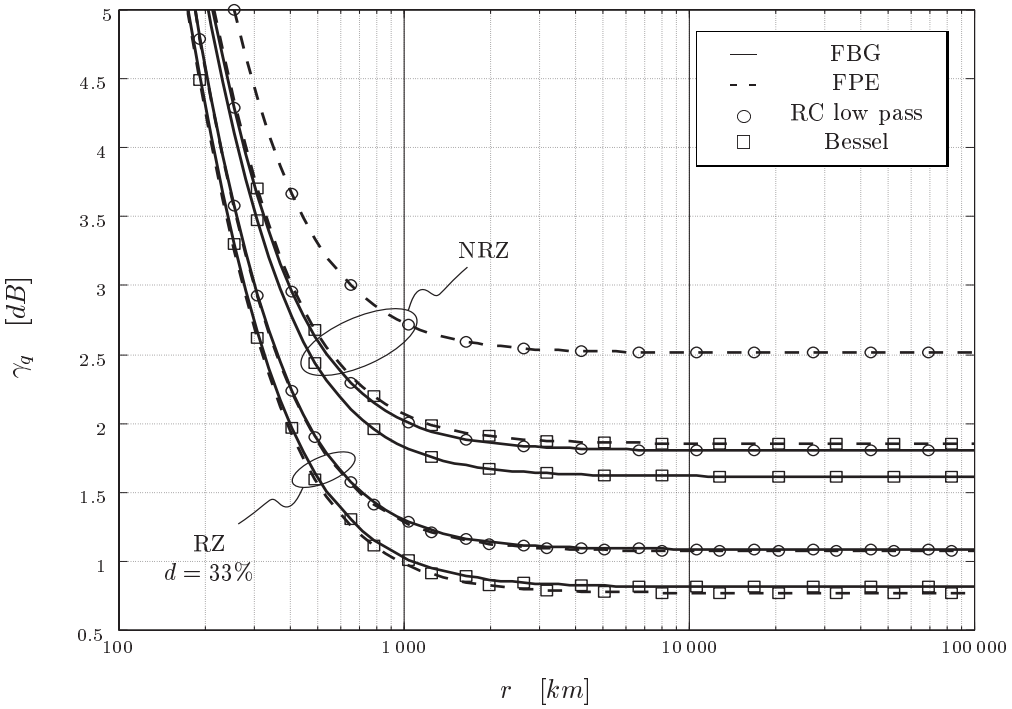

Figure 6. Sensitivity penalty for the different receiver setups vs. satellite link distance.

4.3. Influence of finite extinction ratio

We also investigated the sensitivity degradation due to finite extinction ratios. Figure 7 shows the receiver sensitivity relative to the quantum limit vs. the extinction ratio in dB, $\zeta_{dB} = 10\log(\zeta)$ for the four filter combinations for NRZ as well as for RZ. Typical extinction ratios of about $10dB$ cause sensitivity penalties of $3dB$. For this calculation, the bandwidths were kept to the values optimum for $\zeta = \infty$. Optimizing the filter bandwidths for finite extinction ratios leads to somewhat broader optimum optical filters. This is due to larger '0'-bit noise.[12] On the other hand, a higher tolerance to bandwidth deviations is observed for signals with lower extinction ratios. The curves in Fig. 7 would only be improved by $0.25dB$ when using optimum filter bandwidths.

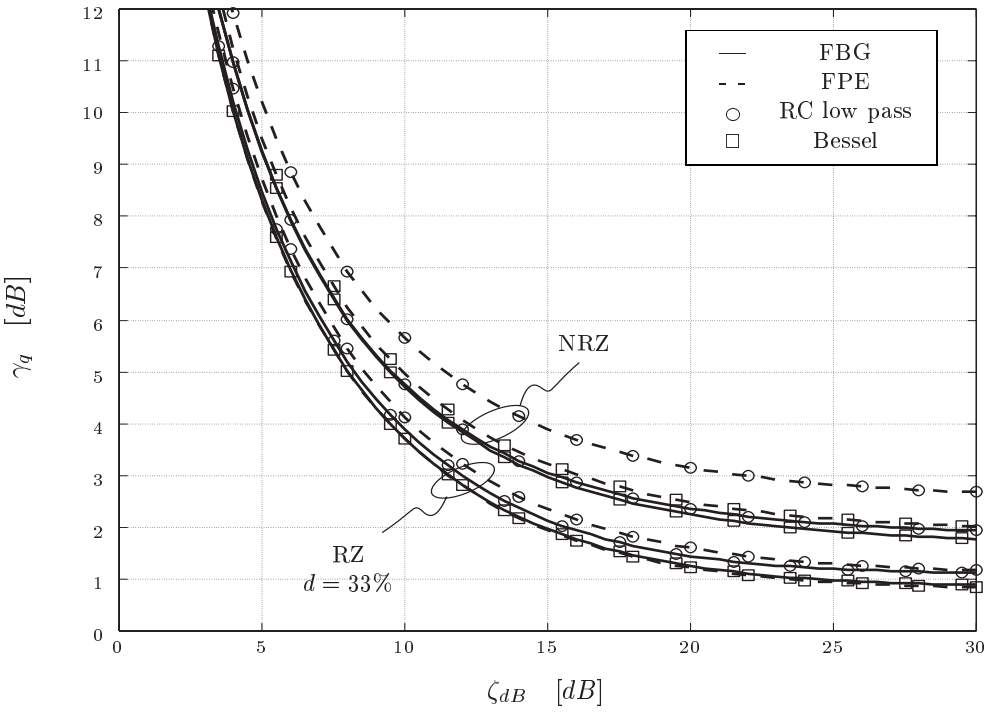

Figure 7. Sensitivity penalty for the different receiver setups vs. extinction ratio.

5. CONCLUSION

We presented simulation results for an optically boosted and optically preamplified on-off keyed system, modeling realistic transmit pulse shapes and filters. The background and ASE noise terms were derived as a function of the link distance.

For the optical filter following the optical preamplifier a bandwidth of 1.5 to 3 times the data rate is optimum with respect to receiver sensitivity. For NRZ coding, fiber Bragg filters are the best choice while for RZ coding Fabry-Pérot filters have a slightly better performance. Receive electronics with a 5^{th} order Bessel characteristic outperform that with a 1^{st} order low pass-like characteristic. The cutoff frequency should not be lower than the data rate. Too narrow filters cause higher penalties than too broad ones.

The influence of link distance on receiver sensitivity was also investigated. For distances larger than several thousand kilometers and antenna diameters of $10cm$ each, the ASE of the booster amplifier is no issue. For shorter distances it is the dominating noise term and causes large sensitivity reductions. The optimum filter bandwidths are unchanged by the influence of the booster ASE.

Reducing the extinction ratio of the transmit signal from its ideal value of infinity strongly reduces the receiver sensitivity. For a realistic value of $10dB$, the received signal power has to be twice as high to achieve the same bit error probability as for the ideal case.

ACKNOWLEDGMENTS

This work was supported by the Austrian Science Fund (FWF) under Project No. P13998TEC and by the Austrian Academy of Sciences under grant 754/99.

REFERENCES

1. O.K.Tonguz, R.E.Wagner, *Equivalence between preamplified direct detection and heterodyne receivers*, IEEE Photon. Technol. Lett. **3**, 835-837, 1991.
2. M.Pauer, P.J.Winzer, W.R.Leeb, *Bit error probability reduction in direct detection optical receivers using RZ coding*, submitted to J. Lightwave Technology.

3. Emmanuel Desurvire, *Erbium-doped fiber amplifiers*, John Wiley & Sons, Inc., 1994.
4. W.R.Leeb, *Degradation of signal to noise ratio in optical free space data links due to background illumination*, Applied Optics **28**, 3443-3449, 1989.
5. P.J.Winzer, A.Kalmar, W.R.Leeb, *Role of amplified spontaneous emission in optical free-space communication links with optical amplification – impact on isolation and data transmission; utilization for pointing, acquisition, and tracking*, Proc. SPIE 3615, Free-Space Laser Communication Technologies XI, January 23-29, 1999, San José (CA/USA), 134-141.
6. B.J.Klein, J.J.Degnan, *Optical antenna gain. 1: Transmitting antennas*, Applied Optics, **13** (9), 2134-2141, 1999.
7. A.Othonos, K.Kalli, *Fiber Bragg gratings: Fundamentals and applications in telecommunications and sensing*, Artec House, Boston, London, 1999.
8. R.Kashyap, *Fiber Bragg gratings*, Academic Press, 1999.
9. D.E. Johnson, *A handbook of active filters*, Prentice Hall, 1980.
10. P.J.Winzer, A.Kalmar, *Sensitivity enhancement of optical receivers by impulsive coding*, J. Lightwave Technol. **17** (2), 171-177, 1999.
11. G.Einarsson, *Principles of lightwave communications*, John Wiley & Sons, Inc., 1996.
12. P.J.Winzer, M.Pfennigbauer, M.M.Strasser, W.R.Leeb, *Optimum bandwidths for optically preamplified (N)RZ reception*, submitted to J. Lightwave Technology, 2000.